The Morphometrical Initiation Stage of the Piezometric Structural Compartment Using Sattelite Imagery in the Southern Slope of Merapi

by Herry Riswandi

International Journal of GEOMATE, Dec., 2019 Vol.17, Issue 64, pp. 217- 223
ISSN: 2186-2982 (P), 2186-2990 (O), Japan, DOI: https://doi.org/10.21660/2019.64.54353
Geotechnique, Construction Materials and Environment

THE MORPHOMETRICAL INITIATION STAGE OF THE PIEZOMETRIC STRUCTURAL COMPARTMENT USING SATTELITE IMAGERY IN THE SOUTHERN SLOPE OF MERAPI

*Herry Riswandi[1, 2], Emi Sukiyah[3], Boy Yoseph CSS Syah Alam[4], and Mohamad Sapari Dwi Hadian[4]

[1]Doctoral Program of Geological Engineering, Universitas Padjadjaran, Bandung; Indonesia
[2]Department of Geological Engineering, Universitas Pembangunan Nasional Veteran, Yogyakarta; Indonesia
[3]Department of Geoscience, Universitas Padjadjaran, Bandung; Indonesia
[4]Department Applied Geology, Universitas Padjadjaran, Bandung; Indonesia

*Corresponding Author, Received: 05 July 2019, Revised: 14 Sept. 2019, Accepted: 26 Oct. 2019

ABSTRACT: The study area is on the southern slope of Merapi Mountain in Yogyakarta, and focus on the relation of satellite imagery with piezometric and structure compartment. The preliminary geological study of satellite imagery is using a digital elevation model and Landsat 8 data extraction. The morphometry initiation is used to get the structure lineaments compartment, and it came from morphometry quantification value to indicating the implication of geological structure controls to the groundwater level distribution. The methods emphasize the quantitative descriptive approach form morphometry equation. Thus quantitative morphometry methods are then follow up by statistical and hierarchical cluster analysis of piezometric. The result of morphometry variable shows the structural lineament creates and control by active tectonics, and it implacable to the piezometric spatial distribution besides the implication of volcanic deposit variation, uplifting and asymmetric river mature form. The statistical analysis represents a relation between structure lineament with the piezometric, and the analysis result imaging on the digitized maps for each compartment compares with the trends of piezometric. The result of this study emphasizes that the initiation of morphometry is needed to use to compartmentation the structure lineaments, and the compartment becomes the controller of piezometric distribution.

Keywords: Morphometry, structure lineament, piezometric, groundwater

1. INTRODUCTION

The crucial stage that happens in the slope of Merapi Mountain as the preserve recharge zone is a morphological change from the wide-opening valley to narrow-closing of the stream. This deformation was causing groundwater level differences with the geological structure to involve. This phenomenon investigates with morphometry initiation using a digital elevation model (DEM) and Landsat 8 imagery data extraction. The extraction is visualizing the remote sensing process in a geographic information system (GIS). This imagery use for the watershed network [1], geological structure lineaments evaluation [2, 3], and it use for piezometric modeling associated with the neotectonic activity reflecting from landform imagery deformation [3, 4, 5]. Morphometry is part of the evaluation of geological structure involvement for structural change on the stream, and the morphology, and it can visualize the variation of piezometric [6].

The streams of Gendol, Opak, Kuning and Boyong is the specific location study objective in the southern slope of Merapi volcanic in Yogyakarta, Indonesia. The lithological unit is depositing on the river's location are composed of young Quarternary pyroclastic rock from the Merapi volcano deposits. The deposits are tuff, ash, breccias, agglomerates, lava, and avalanches deposit [7]. The involvement of these lithological varies responsibility for the changing of the piezometric groundwater level. This changing developed a high-performance solution with morphometry initiation, involving the lineament compartments and piezometric on the pattern of the groundwater flow stage. This research workable to delineate the structural, spatial trend into three different zones. They are analyzing and modifying the different of the piezometric compartment by hierarchical cluster analysis, depicted in the piezometric map and lineament spatial distribution.

2. METHODS

The morphometry and hydrogeological data were analyzing the determination of the existence of the geological structure implication; they also analyze the piezometric groundwater evolution. The statistical relation between piezometric and structural lineament shows in the spatial distribution lineaments and piezometric map. Data management of morphometry and piezometric systematically arranged and aligned into GIS. The extraction data came from the imagery of DEM 30-meter resolution and Landsat 8 imagery data [8] using band 7 for 30-meter and band 8 for 15-meter resolution. The extraction exports to computer-aided design (CAD) and PCI Geomatica to different interpretation data. GIS data constructed to specific information on morphology by calculating the quantitative variables from the surface formation.

The surface information used to determine the value of the geomorphic index, the level of tectonic activity, dimensional aspects such as length and azimuth of river segment, aligned azimuth, flow density, river order, and river ratios, and elevation.

A score of an existing geomorphic index using the formula of each variable, and then used for the analysis of tectonic activity. Bifurcation of the ratio (Rb) is the result of the comparison of the number of a specific order (Σn) river segments with the number of next order (n+1) river segments [9] as in

$$Rb = \frac{\Sigma n}{n+1} \quad (1)$$

Drainage density (Dd) is obtaining by calculating the total length of streamflow (ΣLs) compared to the total watershed area (A) [10] as in

$$Dd = \frac{\Sigma Ls}{A} \quad (2)$$

The sinuosity of mountain front (Smf) is the result of the comparison of the surface length of mountain face (Lmf) to the long straight of mountain face (Ls) [11] as in

$$Smf = \frac{Lmf}{Ls} \quad (3)$$

Valley ratio or comparison of valve width and height (Vf) obtained by comparison of valley width (Vfw) with the height of the right (Eld-Esc) and left valleys (Erd-Esc), as well as the valley ratio elevation [12] as in

$$Vf = \frac{2Vfw}{[(Eld-Esc)+(Erd-Esc)]} \quad (4)$$

The asymmetry factor or the value of river asymmetry (AF) can show the tectonic effect seen from the flow pattern [13, 14]. It can obtain from the comparison of the river basin area (Ar) with the total area (At) of the river basin [15] as in

$$AF = 100 \text{ x } \frac{Ar}{At} \quad (5)$$

The stream length or value of the river gradient index (SL) is deriving from the multiplication of the total length (L) of the river by the ratio of the elevation difference (ΔH) from the point calculated by the length (ΔL) of the river [15] as in

$$SL = \frac{\Delta H}{\Delta L} \text{ x } L \quad (6)$$

Hypsometric integrals (Hi) are calculating the difference in average elevation with minimum elevation, divided by the maximum elevation difference with minimum elevation [16] as in

$$Hi = \frac{H\ mean - H\ min}{H\ max - H\ min} \quad (7)$$

Transverse topographic symmetry (T) is calculating from the ratio of the midline distance from the valley to the maximum height with the diameter spacing from the valley to the minimum height [17, 15] as in

$$T = \frac{Da}{Dd} \quad (8)$$

Elongation of basin ratio (Eb) is obtaining from the ratio of roots to diameter of the circle of the river basin divided by phi, with the length of the watershed [18, 13] as in

$$Eb = \frac{2\sqrt{\frac{Ab}{\pi}}}{lb} \quad (9)$$

The extracted data analyze, including the geological structure such as slope, curvature, aspect, hillshade, lineament, fault, fracture, and piezometric.

This study was using geostatistical analysis to interpret the morphometry and groundwater level spatial distribution, also the influence of groundwater flow and structure involvement. The relation between morphometry and piezometric in the geological structure compartment of the fault is using the hierarchical cluster analysis. Hierarchical cluster analysis using Euclidean distance (space of straight-line calculation from two-point between angle and distance) for same distance measurements. Ward's method for clustering classification, base on the missing information because of object merging to cluster and its measuring use total of square deviation on the mean cluster. It is the Software Statistical Package for the Social Sciences (SPSS) that we used to analyze all samples statistically in piezometric.

Piezometric data mapped by kriging gridding method with Surfer software using a non-directional variogram estimator type. Experimental variograms of piezometric parameters show a sharp curve and linear with spherical variogram component model — the data collected along with the general directions of the regional groundwater flow direction. The data do not tightly cover the entire study area, particularly in the north of a compartment where the data are too rare, and it very close to the top of the volcano. Even the computational technique used for closing the weak data area; there is no other way to make estimating maps for piezometric parameters. The interpretation of interpolation every computed method compares with realizing errors from counting. Comparison of the generated morphometry and piezometric map evaluated in statistical such as maximum, minimum, mean, and variance. All this method were enforced to a geostatistical framework to explain the groundwater piezometric characteristic of the structural compartmentalization.

3. RESULT AND DISCUSSION

The initiate morphometry distribution of watershed flow is assessing by knowing the value of the ratio of bifurcation and drainage density to find out the deformed landform and lithological resistance. Refer to "Eq. (2)" the lower density 3.4 Kuning and 3.9 Opak are indicating a more resistant rock, found in lower reliefs being lightly eroded and having infiltration capacity with good permeability. Density in the Gendol 4.5 can indicate the softer rocks, and Boyong 4.8 indicates a strongly eroded watershed, as shown in Tabel 1.

The Smf calculation refers to "Eq. (3)" from 22 incision relief result minimum number are 1.4 indicates an active tectonic in high level with a full ridge shape, dominant swelling, and erosion, the Smf maximum number are 2.8 is the medium level of tectonic activity.

The Vf calculation refers to "Eq. (4)" results show high uplift level 0.001 to 0.370 and low uplift rate 1.207 to 15.293, counted value less than 0.5 equal to 65% from 22 incision relief, that value indicates the area dominated by high elevation level.

AF calculations refer to "Eq. (5)" in the stream of each with a value of 32.0, 16.7, 31.9, and 19.4, a value less than 50 points indicates a slope due to tectonic movement. The SL calculations "Eq. (6)" on the Gendol show, 5.9 points of value is reflecting the lowest tectonic activity other than Opak 12.2, Kuning 8.6, and Boyong 8.8.

The value of Hi "Eq. (7)" by comparison of elevation (h/H) and river area (a/A) indicates that the integral equations of hypsometry are in the same progression of the mature river, with Gendol 0.407 and 0.480, Opak 0.570 and 0.403, Kuning 0.403 and 0.487, and Boyong 0.426 and 0.415.

The accumulated calculation of the T value "Eq. (8)" shows that the asymmetry value of the river has shifted from the left to the right and has moved towards the West.

The values of Eb calculated "Eq. (9)" from rivers above 0.002-0.004 indicate very elongated, so that river characters classified to tectonically active due to erosion.

The extracted imagery of DEM and Landsat 8 lineaments are analysis using the lighting of azimuth angle, and for the azimuth, straightness showing different directions and does not follow the same pattern. The direction of the azimuth lineaments from DEM 0°-45°-90°-135° show almost has a similar rose diagram with band 7 that higher concentration in the northeast to southwest. DEM 80°-225°-270°-315° shows a higher concentration in the northwest to southeast trend. The azimuth lineaments direction band 8 show east-west, north-south, northeast-southwest, and northwest-southeast trend.

Map of DEM 0°-45°-90°-135°, DEM 80°-225°-270°-315°, Landsat band seven and band 8 shows the classification of lineaments into three sections, which is a draw to the lines of interpretation as structure boundary that cross-cut the lineaments of northeast-southwest direction, as shown in Fig. 1.

Table 1 Morphometric variable to recognize the active tectonic activity.

Morphometry	Stream			
	Gendol	Opak	Kuning	Boyong
Rb	4.3	2.4	2.2	1.5
Dd	4.5	3.9	3.4	4.8
Smf	1.4 to 2.8			
Vf	0.001 to 0.370 and 1.207 to 15.293			
AF	32.0	16.7	31.9	19.4
SL	5.9	12.2	8.6	8.8
Hi	h/H 0.4 a/A 0.5	h/H 0.6 a/A 0.4	h/H 0.4 a/A 0.5	h/H 0.4 a/A 0.4
T	0.65	0.47	0.63	0.87
Eb	0.004	0.003	0.003	0.003

The structure of the compartment had three sections, the northern compartment as a zone A. The central section as a zone B, and the southern section as a zone C. The boundaries of the A zone of the structure compartment are 750-meter to 400-meter elevation. The boundaries of the second B zone of the structure compartment are 400-meter to 300-meter elevation, and C zone of the structure compartment is 300-meter to150-meter elevation.

Hierarchical cluster analysis indicates that the groundwater depth divided into three clusters. This cluster is shown in Fig. 2 on the cluster map and the piezometric pattern in Fig. 3. There was the same interpretation between the structure compartment zone, as shown in Fig. 1, with the division of the piezometric cluster, as shown in Fig. 3.

The structure in each zone A, B, and C corresponds to each cluster one, two, and three piezometric geometry profile. The groundwater table usually follows the local topography [20]. In the profile of topography geometry and piezometric as shown in Fig. 4, groundwater flows from north to south, vertically faulting with normal fault.

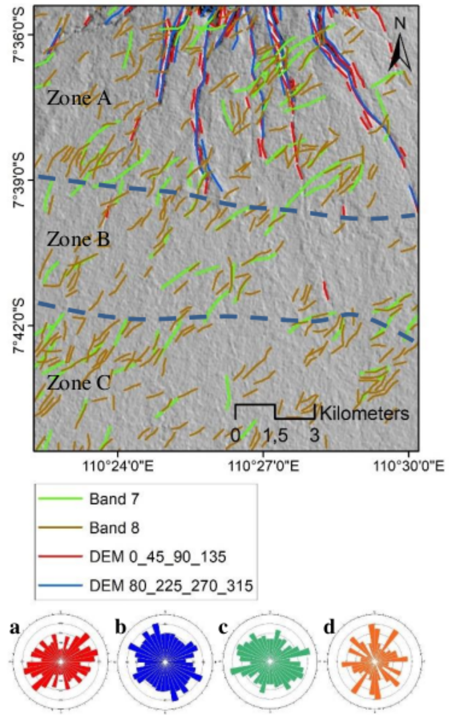

Fig. 1 Lineaments of Landsat and DEM showing the different paths and different direction. Band 7 (a), band 8 (b) DEM 0-45-90-135 (c), and DEM 80-225-270-315 (d), all lineaments trends differently.

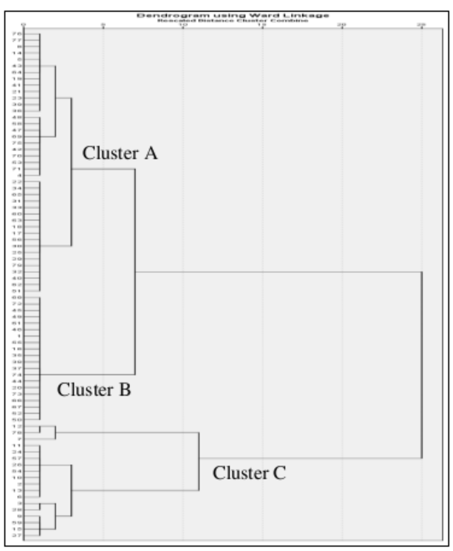

Fig. 2 Dendrogram divided by hierarchical cluster analysis to three clusters.

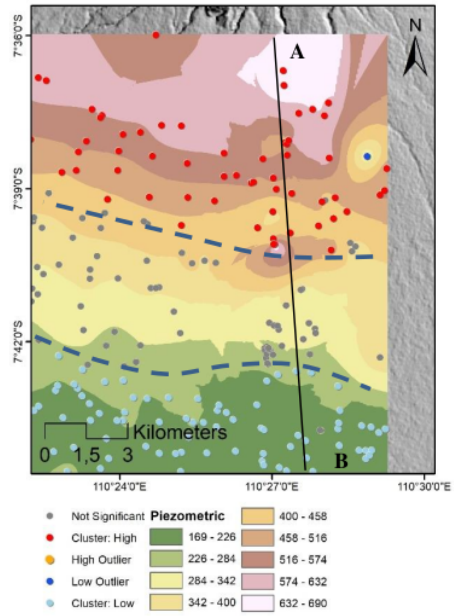

Fig. 3 Piezometric of weighted features, identifies statistically significant groundwater level and spatial outliers using the cluster analysis.

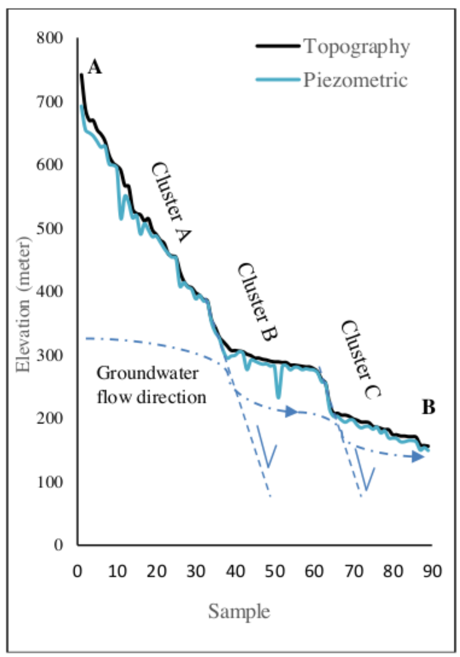

Fig. 4 Profile of topography geometry and piezometric shows divided zone that conformable with structure.

Statistics calculations used for each zone are the minimum and maximum values of depth, and the height of groundwater, the sinuosity of the mountain front (Smf) and the valley ratio (Vf). The value of the relationship between the geological structure with changes in the depth and height of groundwater levels, which then compared with the values of Smf and Vf.

Table 2 Statistics calculations used for each zone are the minimum and maximum values of depth, and the height of groundwater.

Zone		Gendol		Opak	
		Depth	Height	Depth	Height
A	Min	4	4	4	9
	Max	50	64	68	50
B	Min	1	1.2	1	1
	Max	33	50	45	10.9
C	Min	2	1.6	3	2.6
	Max	22	22	10	10

Table 3 Statistics calculations used for each zone are the minimum and maximum values of the mountain front (Smf) and the valley ratio (Vf).

Zone		Smf		Vf	
		Gendol	Opak	Gendol	Opak
A	Min	0.294	0.448	0.021	0.001
	Max	0.550	0.553	40	7.675
B	Min	0.397	0.484	0.711	0.429
	Max	0.533	0.728	10	6.667
C	Min	0.408	0.523	1.052	0.533
	Max	0.476	0.540	14.286	20.571

Zone A Gendol River with a range of values: groundwater depth 4 meters to 50 meters, groundwater level 4 meters to 68 meters, Smf with values of 0.294 to 0.550, Vf with values of 0.021 (high uplift) to 40 (very low uplift). Zone A Opak River with a range of values: depth of groundwater level of 4 meters and a maximum of 68 meters, groundwater level of 9 meters to 50 meters. Smf value of 0.448 to 0.553, Vf value of 0.001 (high uplift) to 7.675 (very low uplift), as shown in Table 2 and Table 3.

Zone B in the Gendol watershed shows the range of values: groundwater depth of 1 meter to 33 meters, groundwater level height of 1.2 meters to 50 meters, Smf value of 0.484 to 0.728, Vf value of 0.711 (moderate uplift) to 10 (low uplift). Zone B in the Opak watershed shows the range of values: groundwater depth 1 meter to 45 meters, groundwater level 1 meter to 10.85 meters, Smf values 0.523 to 0.540, Vf 0.429 (high uplift) to 6.667 (low uplift), as shown in Table 2 and Table 3.

Zone C in the Gendol watershed shows the range of values: groundwater depth of 2 meters to 22 meters, groundwater level height of 1.6 meters to 22 meters, Smf value of 0.408 to 0.476, Vf value of 1.052 (low uplift) to 14.286 (very low uplift). Zone C in the Opak watershed with a range of groundwater depths of 3 meters to 10, groundwater level height of 2.6 meters to 10. Smf values of 0.523 to 0.540, Vf with a minimum value of 0.533 (moderate uplift) and a maximum of 20,571 (very low uplift), as shown in Table 2 and Table 3.

Groundwater flows directions depicted on the piezometric map with the kriging method flowing from the northeast direction with higher elevations to the southwest with lower elevations. The following is an illustration of a piezometric map showing the direction of groundwater flow and groundwater level in each zone.

Groundwater flow follows the direction of the slope of the rock layer, and in the direction of the slope, this shows that the recharge originates from higher elevations, especially from zone A to zone B and continuously to zone C.

Geological structure lineaments act as a boundary toward groundwater flow and lithology slope between different structural divisions. The northeast-southwest-directed structure is a structure used by groundwater flow to connect to the zone above or below, which also functions as a barrier to groundwater flow from north to south.

The results of the ANOVA statistical analysis showed that the groundwater depths of zone A, zone B, and zone C were utterly different. Correlation test results show a reasonably strong correlation between the variable direction of flow and depth of groundwater, and the results of regression tests show the direction of flow and depth of groundwater affect the structure azimuth.

From the ANOVA test, the F count is 12.43 with a significance level or probability of 0.000, a probability of less than 0.05 then the regression model can be used to predict the structure azimuth, or the direction of flow and depth of groundwater affect the structure azimuth, as shown in Table 4.

Table 4 ANOVA with structure azimuth as the dependent variable.

Model	Sum of Squares	df	Mean Square	F	Sig.
Regression	43319.80	2	21659.90	12.43	0.000[a]
Residual	132410.57	76	1742.24		
Total	175730.38	78			

a. Predictors: (Constant), Groundwater depth, groundwater flow.

Table 5 Coefficient with structure azimuth as the dependent variable.

Model	B	Std. Error	Beta	t	Sig.
(Constant)	-3.631	33.009		-0.110	0.913
Flow	30.63	6.635	0.509	4.616	0.000
Depth	0.118	0.410	0.032	0.289	0.774

Regression equation with structure azimuth (Y) is related to the groundwater flow direction (X_1) and groundwater depth (X_2), as in

$$Y = (-3.631) + 30.629 X_1 + 0.188 X_2 \tag{10}$$

A constant of unstandardized coefficients (B) -3.631 states that if the direction of flow is absent or there is no groundwater depth, the azimuth direction of the structure is 3.631°. Regression coefficient X_1 of 30.629 states that any change in groundwater flow direction 1° will change the direction of the structure azimuth by 30.662°. The regression coefficient X_2 of 0.188 states that each additional 1-meter groundwater depth will change the azimuth structure direction of 0.188°, as shown in Table 5.

T-test intent to test the significance of constants and dependent variables (groundwater flow) as seen in the numbers Significance or probability value below 0.025, both significant regression coefficients or groundwater flow direction have a significant effect on azimuth structure, while groundwater depth is not significant.

4. CONCLUSION

The study of the structure compartment on the southern Merapi volcanic slope using a method that combines quantitative morphotectonic with piezometric characteristics. The combination is verified with statistical data analysis to prove that lineament forming due to active tectonic structure.

The morphometry initiation results in the classification of DEM and Landsat lineaments into three sections, as structure boundary that cross-cut the lineaments. The structure compartment had three sections, as a zone A, zone B, and zone C. Also shows the hierarchical cluster analysis classified into three clusters, it has defined the interpretation of spatial dependencies.

The results of a statistical analysis of the ANOVA, correlation test, and regression tests showed every groundwater depths of zone A, zone B, and zone C were utterly different. The direction of flow and groundwater depth have a strong correlation, and it affects the structure azimuth.

The equation of regression $Y = (-3.631) + 30.629 X_1 + 0.188 X_2$, mention that groundwater flow direction has a significant effect on azimuth structure, while groundwater depth is not significant. Any change in groundwater flow direction will change the direction of the structure azimuth. The relationship between groundwater compartments, the structure becomes the controller of the groundwater depth distribution, besides the Quaternary lithology.

5. ACKNOWLEDGMENTS

This paper is part of Doctoral research at Universitas Padjadjaran. The author would like to thank Head of University Padjadjaran for financial support by the 2019 RKDU Scheme and everyone for their help during this research.

6. REFERENCES

[1] P. D. Dinar, Sarino, Y. A.L., J. C. Imroatul and H. S.A., Integration of Surface Water Management in Urban and Regional Spatial Planning, International Journal of GEOMATE, 2018, vol. 14, no. 45, pp. 28-34.

[2] E. Sukiyah, E. Sunardi, N. Sulaksana, and P. P. R. Rendra, Tectonic Geomorphology of Upper Cimanuk Drainage Basin, West Java, Indonesia, International Journal on Advanced Science Engineering Information Technology, 2018, vol. 8, no. 3, pp. 863-869.

[3] X. Shi and B. Xue, Deriving a Minimum Set of Viewpoints for Maximum Coverage Over Any Given Digital Elevation Model Data, International Journal of Digital Earth, 2016, pp. 1-15.

[4] B. Wolosiewicz, Morphotectonic control of the Bialka Drainage Basin (Central Carpathians): Insights from DEM and Morphometric Analysis, Contemp. Trends. Geosci, 2016, vol. 5, no. 1, pp. 61-82.

[5] R. Kaplay, M. Babar, S. Mukherjee, and T. Kumar, Morphotectonic Expression of Geological Structures in The Eastern Part of The South East Deccan Volcanic Province (around Nanded, Maharashtra, India), Tectonics of the Deccan Large Igneous Province, 2016.

[6] A. Petrik and G. Jordan, Systematic Digital Terrain Model Construction And Model Verification With Multi-Source Field Data. Morphotectonic Analysis In The Villany Hills and Its Surroundings, SW Hungary, Carpathian Journal of Earth and Environmental Sciences, 2017, vol. 12, no. 1, pp. 217-224.

[7] B. Bali, A. Wani, R. Khan, and S. Ahmad, Morphotectonic Analysis of the Madhumati Watershed, Northeast Kasmir Valley, Saudi Society for Geosciences, 2016, vol. 9, no. 390, pp. 1-17.

[8] R. Gertisser, S. J. Charbonnier, J. Keller dan X. Quidelleur, The Geological Evolution of Merapi volcano, Central Java, Indonesia, Bulletin of Volcanology, 2012, vol. 74, no. 5, pp. 1213-1233.

[9] G. Buchanan, A. Beresford, M. Hebblewhite, F. Escobedo, H. De Klerk, P. Donald, P. Escribano, L. Koh, J. Martínez-López, N. Pettorelli, A. K. Skidmore, Z. Szantoi, K. Tabor, M. Wegmann, and S. Wich, Free Satellite Data Key to Conservation, Science, 2018, vol. 361, no. 6398, pp. 139-140.

[10] H. T. Verstappen, Applied Geomorphology: Geomorphological Surveys for Environmental Development, New York: Elsevier Science Pub. Co. Inc, 1983, p. 437.

[11] A. Strahler, Quantitative Analysis of Watershed Geomorphology, Transactions, American Geophysical Union, 1957, pp. 913-920.

[12] J. C. Doornkamp, Geomorphological Approaches to the Study of Neotectonics, Journal of the Geological Society, 1986, vol. 143, no. 2, pp. 335-342.

[13] W. Bull and L. D. McFadden, Tectonic Geomorphology North and South of the Garlock Fault, California, in In: Doehring, D.O. (ed.) Geomorphology in Arid Regions Eighth Annual Geomorphology Symposium, New York, 1977.

[14] P. Molin, F. Pazzaglia and F. Dramis, Geomorphic Expression of Active Tectonics in a Rapidly-Deforming Forearc, Sila Massif, Calabria, Southern Italy, American Journal of Science, 2004, pp. 559-589.

[15] R. Kaplay, M. Babar, S. Mukherjee, and T. Kumar, Morphotectonic Expression of Geological Structures in The Eastern Part of The South East Deccan Volcanic Province (around Nanded, Maharashtra, India), Tectonics of the Deccan Large Igneous Province, 2016.

[16] E. Keller and N. Pinter, Active Tectonics. Earthquakes, Uplift, and Landscape, 2nd ed., New Jersey: Upper Saddle River, N.J.: Prentice-Hall, c2002, 1996, p. 362.

[17] R. J. Pike and S. E. Wilson, Elevation-Relief Ratio, Hypsometric Integral, and Geomorphic Area-Altitude Analysis, Bulletin of the Geological Society of America, 1971, vol. 82, no. 4, pp. 1079-1084.

[18] R. T. Cox, Analysis of Drainage-Basin Symmetry as a Rapid Technique to Identify Areas of Possible Quaternary Tilt-Block Tectonics: An example from the Mississippi Embayment, The Geological Society of America Bulletin, 1994, vol. 106, no. 5, pp. 571-581.

[19] S. A. Schumm, Evolution of drainage system and slope badlands at Perth Amboy, New Jersey, Geological Society of America Bulletin, 1956, vol. 67, no. 5, pp. 597-646.

[20] T. L. R.A., N. Sulaksana, B. Y. CSSSA and A. Sudradjat, Topographic Control on Groundwater Flow in Central of Hard Water Area, West Progo Hills, Indonesia, International Journal of GEOMATE, 2019, vol. 17, no. 60, pp. 83-89.

The Morphometrical Initiation Stage of the Piezometric Structural Compartment Using Sattelite Imagery in the Southern Slope of Merapi

ORIGINALITY REPORT

8%	7%	3%	2%
SIMILARITY INDEX	INTERNET SOURCES	PUBLICATIONS	STUDENT PAPERS

PRIMARY SOURCES

1	Submitted to Kirkuk University Student Paper	1%
2	repository.unp.ac.id Internet Source	1%
3	ijsr.net Internet Source	1%
4	en.earth-science.net Internet Source	1%
5	biakom.com Internet Source	1%
6	Abdelhakim Jilali, Yassine Zarhloule. "Structural control of the hydrogeology in Figuig Oasis in the eastern High Atlas of Morocco", Proceedings of the Geologists' Association, 2015 Publication	<1%
7	uir.unisa.ac.za Internet Source	<1%

8 www.ijsrst.com
Internet Source
<1 %

9 Dewandra Bagus Eka Putra, Mohamad Sapari Dwi Hadian, Boy Yoseph CSS Syah Alam, Yuniarti Yuskar et al. "Groundwater study in coastal region: Geochemistry and saltwater intrusion analysis of an island in Malacca Strait, Indonesia", Environmental Engineering Research, 2020
Publication
<1 %

10 Mohammad Moumeni, Reza Nozaem, Maryam Dehbozorgi. "Quantitative assessment of the relative tectonic activity using the analytical hierarchy process in the northwestern margin of the Lut Block, Central Iran", Journal of Asian Earth Sciences, 2020
Publication
<1 %

11 Parul N. Joshi, D.M. Maurya, L.S. Chamyal. "Morphotectonic segmentation and spatial variability of neotectonic activity along the Narmada–Son Fault, Western India: Remote sensing and GIS analysis", Geomorphology, 2013
Publication
<1 %

12 core.ac.uk
Internet Source
<1 %

13 iarjset.com
Internet Source

		<1%
14	ijsrst.com Internet Source	<1%
15	journalijpss.com Internet Source	<1%
16	rebus.us.edu.pl Internet Source	<1%
17	tel.archives-ouvertes.fr Internet Source	<1%
18	www.intechopen.com Internet Source	<1%

Exclude quotes	On	Exclude matches	< 5 words
Exclude bibliography	On		